RSC Advances

PAPER

View Article Online
View Journal | View Issue

Cite this: *RSC Adv.*, 2017, **7**, 34307

Wash-free colorimetric homogeneous immunoassay for *Zygosaccharomyces rouxii*†

Hong Guo, Ya Hong Yuan, Chen Niu, Zhouli Wang, Yue Qiu and Tian Li Yue *

Received 7th March 2017
Accepted 15th June 2017

DOI: 10.1039/c7ra02791e

rsc.li/rsc-advances

Convenient, rapid and reliable detection of food spoilage microorganisms has always been critical to food safety. Commonly used methods such as an enzyme-linked immunosorbent assay (ELISA) often rely on tedious wash steps and incubation procedures. A convenient two-step colorimetric homogeneous immunoassay strategy for rapid visual detection of *Zygosaccharomyces rouxii*, which efficiently simplified the immunoassay process, was developed. Immunogold nanospheres (Ab–PEG–AuNPs) were used as specific colorimetric probes. The proposed method depends on adjusting the interparticle spacing of Ab–PEG–AuNPs on the cell surface of *Z. rouxii*, leading to a visible color change. This simple method exhibits good sensitivity and specificity which depends on the characteristic of Ab against *Z. rouxii*, and the detection results are in great agreement with those of ELISA. Moreover, the method is successfully applied to detect *Z. rouxii* in apple juice.

Introduction

The rapid and accurate analysis of food spoilage microorganisms is very important for food safety. Methods such as ELISA that depend on antibody–antigen interactions are widely used for food microbiology analysis.[1–7] Despite considerable advances in food spoilage microorganism detection with enhanced sensitivity, current immunoassay methods present some drawbacks. First, antigens or capture antibodies are randomly immobilized on a two-dimensional surface, which often leads to insufficient capture of target microorganisms, thereby possibly impacting detection sensitivity.[8] Second, tedious wash steps are inevitable in conventional ELISA or plastic ELISA, which are time consuming.[1,2,9] Third, the enzymes involved are often sensitive to environmental conditions, which restricts the application fields.

Due to the high extinction coefficients of AuNPs, they have been used in homogeneous colorimetric assays to detect a large amount of analytes such as DNA, ions, and small organic compounds.[10–12] Colorimetric assays are advantageous in that their readouts are simple and can even be observed by the naked eye without any expensive equipment. In comparison with conventional immunoassays, the colorimetric immunoassay simplifies the assay process and increases sensitivity without requiring separation steps. The targets that induce AuNP aggregation cause an evident optical transition resulting in a red-to-blue color change. In general, the cross-linked AuNPs–targets–AuNPs lead to an evident optical transition when the inter-spacing of AuNPs–targets–AuNPs is smaller than the diameter of individual AuNPs. However, there is a limit for the detection of larger targets when the inter-spacing of AuNPs–targets–AuNPs is larger than the diameter of individual AuNPs. Thus, Liu *et al.*[8] reported a homogeneous colorimetric assay, wherein the growth of AuNPs could be controlled to decrease the inter-particle spacing of AuNPs–protein–AuNPs. With the addition of Au growth solution, the enlargement of particle size may decrease the inter-particle spacing of the cross-linked AuNPs–protein–AuNPs, thus inducing a distinct optical transition to detect larger proteins. However, this simple method could be limited to detect larger microbes because the inter-spacing of AuNPs–microbe–AuNPs is much larger than that of cross-linked AuNPs–protein–AuNPs.

Thus, we developed the concept of Liu *et al.*[8] using specific polyclonal antibodies against microbes to recognize numerous binding sites on the surface of microbes. Therefore, Ab–PEG–AuNPs can be focused on the surface of microbes with a closer inter-particle spacing. The microorganism *Zygosaccharomyces rouxii* has an extreme tolerance to sugar and salt, and it has long been considered a major contributor to food spoilage.[13–15] Hence, we herein used polyclonal *Z. rouxii* antibodies, which recognize a large amount of cell surface antigens of *Z. rouxii*, to enrich AuNPs. Upon addition of Au growth solution, Au particles become larger on the yeast cell surface, which may decrease the inter-particle spacing of the AuNPs on the cell surface of *Z. rouxii*, leading to a distinct optical transition (Fig. 1). Finally, we establish a wash-free homogenous colorimetric immunoassay for detection of *Z. rouxii* in apple juice.

College of Food Science and Engineering, Northwest A&F University, Yangling 712100, China. E-mail: yuetl305@nwsuaf.edu.cn; ytl6503@163.com; Fax: +86-29-87092492; Tel: +86-29-87092492

† Electronic supplementary information (ESI) available. See DOI: 10.1039/c7ra02791e

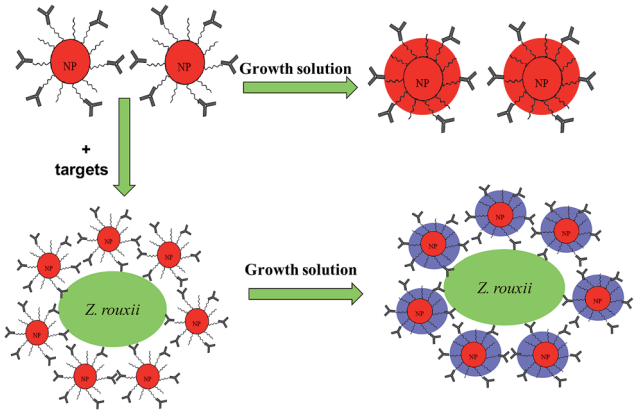

Fig. 1 Schematic of wash-free immunoassay based on the growth of AuNPs.

Materials and methods

Reagents, materials and instrumentation

Hydroxylamine (NH_2OH), gold(III) chloride trihydrate ($HAuCl_4 \cdot 3H_2O$), *N*-hydroxysuccinimide (NHS), bovine serum albumin (BSA), goat anti-rabbit IgG–horseradish peroxidase (GAR–HRP), 3,3′,5,5′-tetramethyl benzidine (TMB) (St. Louis, Mo., U.S.A.), and PEG 2000 derivative (H_2N–PEG–COOH) were purchased from Sigma. Trisodium citrate, thioctic acid, PBS (pH 7.4), and 4-dimethylaminopyridine (DMAP) of high purity were purchased locally. ELISA was carried out in 96-well polystyrene microplates (Nunc, Roskilde, Denmark). The UV-vis spectra were recorded with U-2500 spectrophotometer (Shimadzu). The absorbance of AuNP solutions in 96-well microplates was observed at 528 nm. TEM images were obtained using a JEOL1230 TEM at an accelerating voltage of 100 kV.

Preparation of antigen

The strain *Z. rouxii* B-WHX-12-54 used in this study was previously isolated from apple juice concentrate[16] and was cultured in YPD medium (1% yeast extract, 2% bacto-peptone and 2% glucose) and 60% YPD medium (1% yeast extract, 2% bacto-peptone and 60% glucose)[17] at 28 °C and 120 rpm for 48 h. Yeast cells grown in 60% YPD medium (h-*Z. rouxii*) were harvested by centrifugation and washed three times with sterile water, and the final cell concentration was approximately 1×10^9 CFU mL^{-1}. The antigens were stored at −20 °C until use.[18]

Preparation of immunogold colorimetric probe

Antibody production. Immunization was performed according to reported methods.[19] Briefly, two New Zealand White male rabbits were inoculated by ear-vein intravenous injection with 1 mL antigen (*Z. rouxii* cells) at 10^9 CFU mL^{-1}, followed by injection of 2 mL antigen on six subsequent occasions at four-day intervals. After the final immunization, the serum of the inoculated rabbits was collected and pretreated by a saturated ammonium sulfate (SAS) precipitation method. The polyclonal antibody (Ab) was purified and then divided into aliquots and finally stored at −20 °C.[18]

Treated polyclonal antibody (tAb) was prepared by the methods described by Casanova[20] with minor modifications. Briefly, the Ab was adsorbed three times with 6 mg dried heat-killed *Z. rouxii* B-WHX-12-54 grown in YPD medium (l-*Z. rouxii*) and stored at −20 °C until used. The animal protocol was approved by the laboratory animal management committee of Shanghai. All of the experimental procedures followed the Guide for the Care and Use of Laboratory Animals: eighth edition, ISBN-10: 0-309-15396-4. The housing facility was a barrier housing facility, and it met the criteria laid out by the National Standard of China, Laboratory Animal-Requirements of Environment and Housing Facilities (GB 14925-2010/XG1-2011). All efforts were made to minimize animal suffering. Informed consent: not applicable.

Synthesis of gold nanoparticles. Citrate coated gold nanoparticles were synthesized using the Turkevich method[21] as reported in a previous study. Briefly, to a boiling solution of 100 mL $HAuCl_4$ (0.01% w/v), 5 mL 1% trisodium citrate was added. After boiling for 10 min, the solution was cooled to the room temperature for use.

Synthesis of PEG linker. The PEG linker was synthesized according to the method recently described by Liu.[8] Briefly, 0.67 g thioctic acid was added into 10 mL anhydrous dichloromethane containing 0.45 g NHS while stirring. Then, EDC–HCl (0.69 g) and catalyst DMAP (~0.2 g) were added. The mixed solution was cooled for 1 h and allowed to react overnight at room temperature. The resulting solution was diluted with dichloromethane (15 mL) and washed with saturated brine (25 mL) several times. Then, the mixture was dried using Na_2SO_4 to produce an NHS-activated ester. The activated ester (91 mg) was added to a solution of H_2N–PEG–COOH (0.5 g) in dichloromethane (15 mL) and stirred, and the solution was left to react overnight. The obtained solution was concentrated to 5 mL and then cold diethyl ether (25 mL) was added dropwise to obtain a precipitate. Finally, we obtained a PEG linker in which one side of the heterobifunctional H_2N–PEG–COOH reacted with thioctic acid and the other side was carboxylic acid activated by *N*-hydroxysuccinimide (NHS).

Synthesis of Ab–PEG–AuNP colorimetric probe. 10 mL as-prepared AuNP was incubated with 0.003 g PEG linker at room temperature for 2 h. The mixture was purified by centrifugation (1100 rpm, 20 min) and resuspended twice in PBS. Then, 4 mL of the purified solution was incubated with 16 μL h-*Z. rouxii* polyclonal antibody (6.3 mg mL^{-1}) at 4 °C overnight. In order to hydrolyse the unspecific site of NHS, 0.2 mL PBS (pH 8.5) was added. Then, Ab–PEG–AuNPs were purified by centrifugation and resuspended in ultra-pure water to form a colorimetric probe stock solution.

Procedure of wash-free colorimetric immunoassay for *Z. rouxii* detection in PBS buffer

The wash-free immunoassay was used to detect *Z. rouxii* by two steps without washing. In the first step, the as-prepared Ab–PEG–AuNP colorimetric probe (diluted to 1 nM) was incubated

with *Z. rouxii* at 37 °C for 30 min. Second, Au growth solutions 10 μL NH_2OH (400 mM; pH, 5) and 8 μL $HAuCl_4$ (0.1 w/v%) were added to the analysis system. The color of the Ab–PEG–AuNP solution changed from light pink to red or blue. AuNP growth is a dynamic process and leads to increasing color intensity with time. As AuNPs usually precipitate absolutely after 120 s, visible color changes were recorded within 25–120 s. To ensure consistency of results, all the wash-free immunoassay photos were taken within 25–120 s.

ELISA analysis

The procedure used for ELISA analysis was according to that provided by Wang *et al.*[22] with minor modifications. In our process, 96-well microtiter plates were coated with 100 μL sample for 1 h at 37 °C. After incubation, the plates were washed three times with 200 μL 10 mM PBS (pH 7.4) with 0.05% Tween-20. Then, the plates were incubated with blocking buffer, 5% milk powder in 10 mM PBS at 37 °C, for 2 h (200 μL per well). After three washes, the wells were blotted on adsorbent paper. Then, 100 μL of diluted antibody (1 : 4000 in PBS) was added. Following additional incubation for 1 h at 37 °C, the plate was washed again. GAR–HRP was then added (1 : 2000 in PBS; 100 μL per well) and the plate was incubated at 37 °C for 1 h. After three washes, substrate solution A (3,3′,5,5′-tetramethylbenzidine (TMB)) and substrate solution B (0.03% H_2O_2) were added to each well (100 μL) to allow color development for 15 min under dark conditions at 37 °C. The reaction was stopped by adding 50 μL of sulfuric acid (2 M). The optical density of each well was measured at 450 nm by a microtiter plate reader (Bio-Rad Laboratories. Inc. Hercules. CA. USA).

Immunofluorescence studies

The method of immunolabeling of *Z. rouxii* grown under different sugar stresses (10%, 20%, 30%, 40% and 60% YPD media) was according to that reported by Beaussart *et al.*[23] Images were obtained using an Andor CSU-W confocal microscopy system. A 100× oil objective with a DU-888U3-CSO was used for all images that were captured with Andor iQ3 live cell imaging software.

Apple juice samples

The *Z. rouxii* B-WHX-12-54 was cultured in YPD at 28 °C for 48 h to produce working stock solution and stored at 4 °C for routine use. Moreover, 100 μL of cells from the working stock solution were incubated into 12° Brix, 25° Brix, 34° Brix, 42° Brix, and 59° Brix apple juice and allowed to grow. The apple juice samples were then detected using the wash-free immunoassay based on AuNPs.

Live subject statement

The animal protocol was approved by the laboratory animal management committee of Shanghai. All of the experimental procedures followed the Guide for the Care and Use of Laboratory Animals: eighth edition, ISBN-10: 0-309-15396-4.

Results and discussion

Principle of wash-free immunoassay

We developed the concept of immunoassay protein, as reported by Liu *et al.*[8] to qualitatively detect larger microbes. The principle of the established immunoassay method in this study to detect microbes is summarized in Fig. 1. To investigate the feasibility of the wash-free colorimetric immunoassay, we prepared AuNPs and a PEG linker. One of the side of PEG linker containing a dithiol group was functionalized onto AuNPs surface *via* Au–S to form PEG–AuNPs. AuNPs and Ab–PEG–AuNPs can be used as seeds to grow larger AuNPs by addition of Au growth solutions (NH_4OH and $HAuCL_4$).[8] To confirm this, the growth of AuNPs and PEG–AuNPs was first investigated. In this study, AuNPs and PEG–AuNPs were diluted 5 fold in Milli Q water (about 1 nM) and added to Au growth solution (NH_4OH (10 μL) and $HAuCL_4$ (8 μL, 0.01% w/v)). As indicated in Fig. S2,† AuNPs contain several cross-linked aggregates, while PEG–AuNPs show mostly individual NPs, indicating the role of the PEG linker in dispersion formation. After introduction of Au growth solutions, the resulting solutions of AuNPs became blue, and the color of PEG–AuNP solutions turned red. Corresponding TEM images of AuNPs showed undesirable aggregates (Fig. 2c), while PEG–AuNPs exhibited good dispersion (Fig. 2d). The synthetic AuNPs in PEG–AuNPs with a diameter of about 13 nm at 200 000× magnification display spherical morphology and grow to about 30 nm after addition of Au growth solutions. The highly stable dispersions of PEG–AuNPs were consistent with those observed in a previous study, which showed that PEGylated gold nanoparticle bioconjugates form highly stable dispersions.[24] Therefore, PEG–AuNPs were selected to prepare the colorimetric probe for further study.

We then used the PEG–AuNPs to conjugate Ab to establish the AuNP-based immunoassay. Ab is usually stored at −20 °C to maintain its good biological activity. As the formation of Ab-conjugated PEG–AuNPs requires only two simple steps, we evaluated the stability of PEG–AuNPs. After storage of the PEG–AuNPs in a refrigerator for several months at 4 °C, we were able to obtain the same results as shown in Fig. S2,† which indicate high stability and shelf life of the conjugates. PEG–AuNPs were stored at 4 °C for routine use. In this study, polyclonal antibodies against *Z. rouxii* (Ab) were obtained. Ab was then conjugated with the PEG–AuNPs by means of amide bonds to form Ab–PEG–AuNPs. Fig. 2 shows the step-by-step modification of AuNPs. As shown in Fig. S1,† after conjugation with Ab, the absorbance peak of AuNPs red-shifts from 518 nm to 522 nm. The difference of the resonance peak is due to the local increase in the reflective index caused by the addition of antibody layers.[25] This information indicates the successful preparation of Ab–PEG–AuNPs.

Herein, specific polyclonal antibodies were used to recognize the cell surface antigens of target microbes, with AuNPs act as the signal indicator. PEG is used to stabilize AuNPs to prevent their aggregation. Thus, Ab specifically recognizes *Z. rouxii* and subsequently anchors Ab–PEG–AuNPs complexes on it (Fig. 1). The Ab–PEG–AuNPs will disperse in the absence of the target

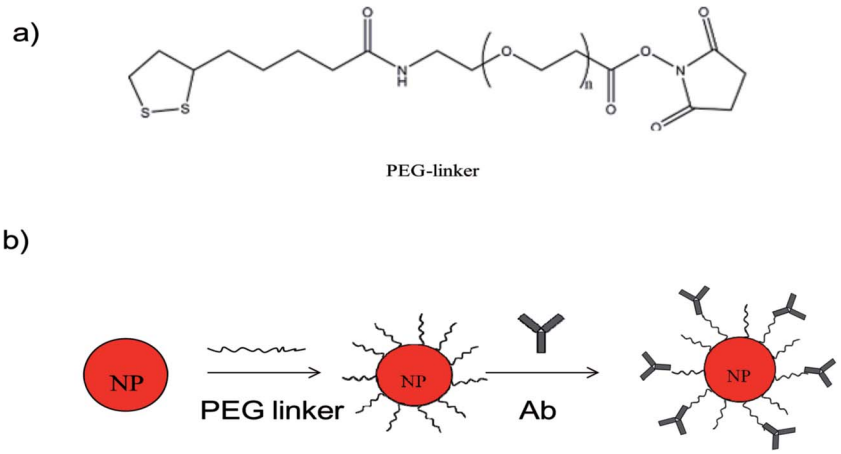

Fig. 2 (a) Structure of PEG linker; (b) step-by-step assembly of Ab–PEG–AuNPs.

strain and will focus on the cell surface of *Z. rouxii*. At this time, enrichment of AuNPs on the surface of *Z. rouxii* does not cause a color change because the inter-particle distance of AuNPs is still larger than the diameter of individual AuNPs.[8] After the introduction of growth solutions to the analysis system, the diameter of individual AuNPs increased to around 30 nm with dispersion, which was similar to the result shown in Fig. 2d in the absence of a target, resulting in a deep-red solution. In contrast, when the *Z. rouxii* B-WHX-12-54 is present in the Ab–PEG–AuNP solution, the forming of large-sized AuNPs may decrease the inter-particle spacing of AuNPs on the cell surface of *Z. rouxii* with large-scale aggregation, resulting in a blue color.

Wash-free colorimetric immunoassay for *Z. rouxii* detection in PBS

We now investigate the detection of *Z. rouxii* B-WHX-54 in PBS (pH 7.4). First, blank PBS (3 μL) and 10^5 CFU mL^{-1} *Z. rouxii* B-WHX-12-54 (3 μL) were incubated with Ab–PEG–AuNP solution (600 μL, 1 nM) at 37 °C for 30 min. The color and maximum absorption peak of the analysis system were not significantly changed (Fig. 3a and b). It has been reported that the mixing of small biological molecular targets with Ab–AuNPs would cause cross-linking of Ab–AuNP probes to form aggregates, leading to a red-shift.[11,12,23] The different results between the larger microorganisms and small analyte is due to the inter-particle

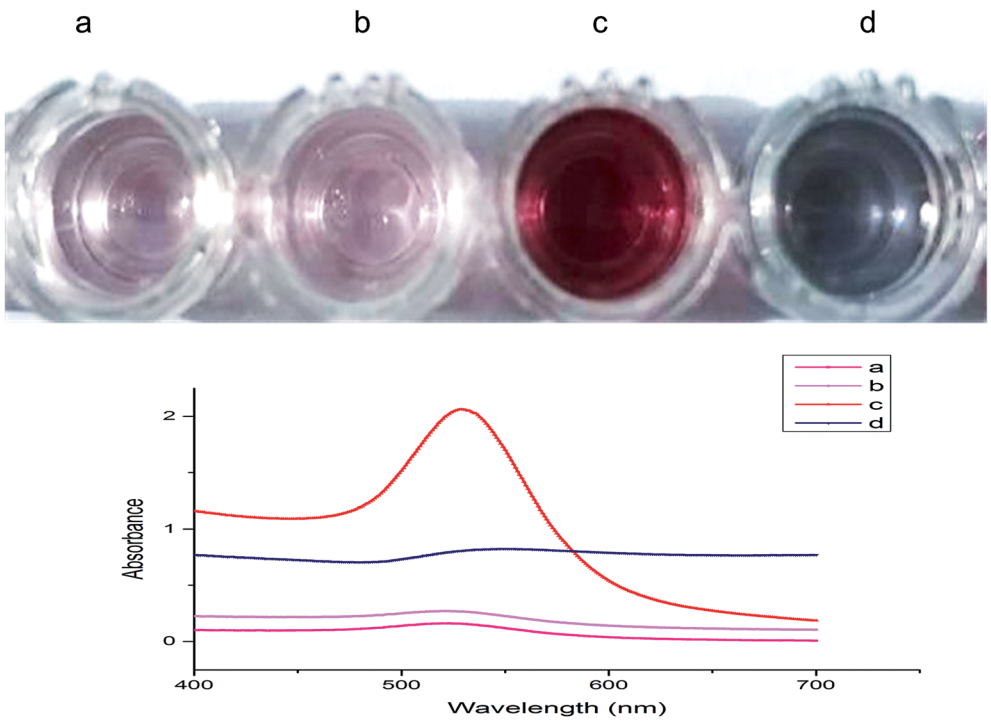

Fig. 3 UV-vis spectra and corresponding photographs of analytical solutions. (a) Ab–PEG–AuNP; (b) (a) incubated with *Z. rouxii*; (c) (a) +Au growth solution; (d) (b) +Au growth solution.

spacing of AuNPs. After addition of Au growth solutions, Ab–PEG–AuNPs grow into a larger-sized AuNPs with dispersions in the absence of targets, resulting in a deep-red solution (Fig. 3c). The corresponding absorbance at 528 nm increased from 0.161 to 2.063. This is because the free dispersion of Ab–PEG–AuNPs does not decrease the inter-particle spacing of AuNPs. Conversely, the introduction of growth solutions to the Ab–PEG–AuNPs–*Z. rouxii* complex caused AuNP aggregation, resulting in a blue solution (Fig. 3d). We speculated that the growth of AuNPs decreases the interparticle spacing of the Ab–PEG–AuNPs on the surface of the *Z. rouxii*, which was verified by a distinct wavelength red-shift of SPR. As a result, the absorption band shifted from 528 nm to 554 nm with increased SPR intensity. Undoubtedly, this method can detect spoilage yeast by mixing sample and colorimetric probe followed by introduction of Au growth solutions, without the involvement of any enzymes and tedious wash steps.

Sensitivity, specificity and reliability of wash-free immunoassay

The sensitivity of the wash-free colorimetric immunoassay for *Z. rouxii* detection was evaluated in PBS (pH 7.4). The Ab–PEG–AuNPs (diluted to 1 nM) were incubated with various amounts of h-*Z. rouxii* B-WHX-12-54 and l-*Z. rouxii* B-WHX-12-54 cells with final concentrations of 10^1, 10^2, 10^3, and 10^4 CFU mL^{-1} in PBS at 37 °C for 30 min. On addition of Au growth solutions, as indicated in Fig. 4a, the color changed to blue when the analytical system contained10^3 CFU mL^{-1} of h-*Z. rouxii* B-WHX-12-54. The color change was measured by absorbance at 528 nm. By plotting $-\Delta A_{528}$ ($-\Delta A_{528} = A - A_0$, where A is the absorbance of the Ab–PEG–AuNP solution at 528 nm after adding targets and Au growth solutions and A_0 is that of the blank sample) *versus* various concentrations of *Z. rouxii*, Fig. 4b was achieved. The results indicated that the colorimetric probe is sensitive to *Z. rouxii* B-WHX-54. However, the polyclonal h-*Z. rouxii* antibody showed a different affinity for sensing *Z. rouxii*, being able to sense 10^3 CFU mL^{-1} of h-*Z. rouxii* and 10^4 CFU mL^{-1} of l-*Z. rouxii*. One of the reasons could be that the affinity of the antibody is related to the analyte structure.[26,27] Since stress conditions can affect the structure of microorganisms,[28] Ab could have different affinity to *Z. rouxii* grown under different stresses. Another reason could be that the cell proteins usually change when subjected to sugar stress. Kim *et al.*[29] have suggested that *Candida magnoliae* grown in 300 g L^{-1} glucose medium will cause protein changes. Recently, we also demonstrated that *Z. rouxii* grown in a high sugar content medium (600 g L^{-1} glucose) will vastly reprogram proteins.[17]

Subsequently, the specificity of the wash-free immunoassay was tested *via* incubation of analysis solutions with h-*Z. rouxii*, l-*Z. rouxii*, *Zygosaccharomyces bailii*, *Debaryomyces hansenii*, *Hanseniaspora uvarum*, and *Saccharomyces cerevisiae*. Except h-*Z. rouxii*, all test strains were grown in YPD media and washed with PBS. Upon addition of Au growth solutions, only h-*Z. rouxii* and l-*Z. rouxii* displayed a blue colour (Fig. 5a), and the adsorption peaks shifted significantly (Fig. 5b), suggesting the high selective performance of the probe.

Before applying the AuNP-based method to detect different concentrations of apple juice (different sugar content), we immunostained *Z. rouxii* B-WHX-54 under different sugar stress conditions (Fig. 6). Although the morphology of *Z. rouxii* B-WHX-54 significantly changed, homogeneous fluorescence was found on the cell surface of *Z. rouxii* B-WHX-54, which suggested that Ab could identify several binding sites on the surface of *Z. rouxii* B-WHX-54. These results confirm the reliability of the principle of the wash-free colorimetric immunoassay.

Detection of *Z. rouxii* in apple juice

With these promising results, this method was applied to detect *Z. rouxii* B-WHX-12-54 in apple juice. *Z. rouxii* B-WHX-12-54

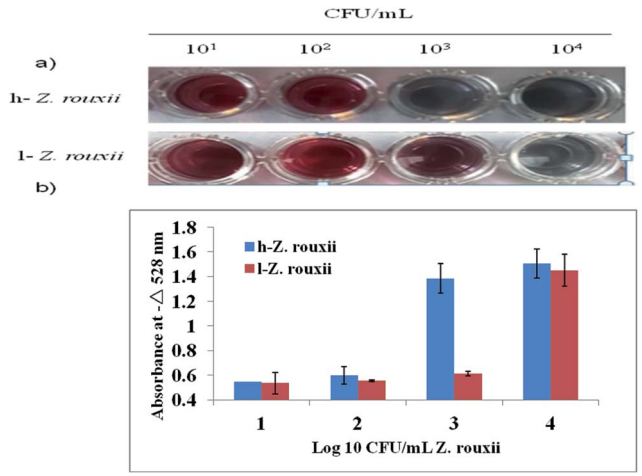

Fig. 4 Photographs (a) and typical absorption spectral response (b) of wash-free immunoassay at various concentrations of *Z. rouxii*. Error bars denote the standard deviation of the absorbance values from the three replicate assays.

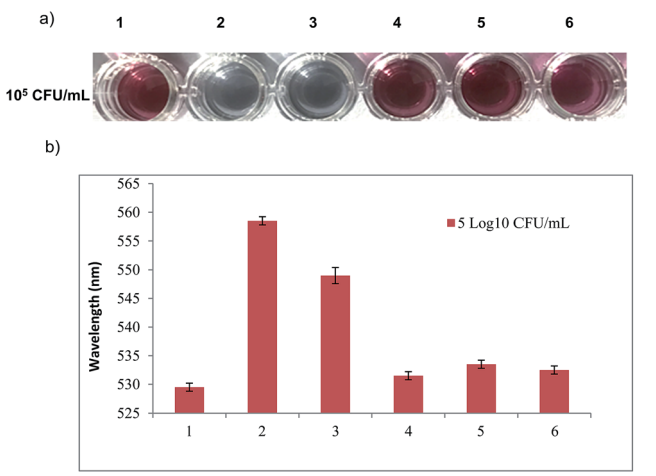

Fig. 5 Photographs (a) and typical absorption spectral response (b) of wash free immunoassay various tested strains. 1 blank, 2 h-*Z. rouxii*, 3 l-*Z. rouxii*, 4 *Z. bailli*, 5 *D. hansenii*, 6 *S. cereviae*. Error bars in (b) denote the standard deviation of the wavelength.

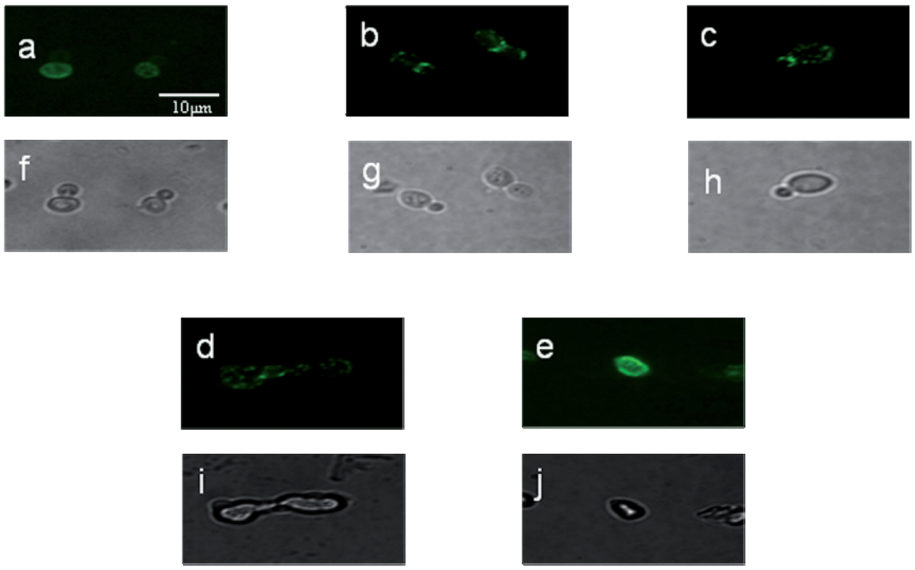

Fig. 6 Fluorescence imaging of *Z. rouxii* B-WHX-12-54 grown at different sugar concentrations. Fluorescence (a–e) and phase-contrast (f–j) images of *Z. rouxii* BW-WHX-12-54 grown in 10%, 20%, 30%, 40% and 60% YPD media, stained with anti-*Z. rouxii* pAb, followed by FITC-conjugated secondary antibodies.

grown at different concentrations of apple juice (12° Brix, 25° Brix, 34° Brix, 42° Brix, and 59° Brix) was incubated with Ab–PEG–AuNP solutions with final yeast concentrations of 0, 10^3, 10^4, and 10^5 CFU mL^{-1}. As indicated in Fig. S3,† the wash-free method can be used for detecting *Z. rouxii* in 12° Brix apple juice, while the detection was seriously disturbed in 25–59° Brix apple juice. The reason could be that the polyclonal antibodies can cross-react with antigenic matrix in apple juice.

To reduce the cross-reactivity of the antibody, Casanova *et al.*[20] demonstrated that *C. albicans* polyclonal antibodies were adsorbed with blastoconidia to avoid cross-reaction of the latter. Therefore, we try to obtain the treatment antibody (tAb) using l-*Z. rouxii* to adsorb Ab and evaluate whether it can avoid cross-reaction. Then, the obtained tAb is used for the synthesis of tAb–PEG–AuNP probes, as described in the materials and methods. We then use the tAb–PEG–AuNP solution to detect *Z. rouxii* B-WHX-12-54 at different concentrations of apple juice. The results in Fig. 7 showed that tAb–PEG–AuNPs can be used for detection of 12–42° Brix apple juice. Detection limit was determined to be 10^4 CFU mL^{-1} of *Z. rouxii* in 42° Brix apple juice and 10^5 CFU mL^{-1} of *Z. rouxii* in apple juice with concentration ranging from 12 to 34° Brix, which led to visible color changes. The reason may be that the tAb avoids the cross-reaction of food matrix in apple juice because some cell surface antigenic compositions of l-*Z. rouxii* may be similar to sugar compositions in apple juice. Therefore, these polyclonal antibodies, which cross-react with apple juice, are removed by adsorption of l-*Z. rouxii*. These results suggest that the adsorbed antibodies facilitate the wash-free immunoassay method to detect *Z. rouxii* in a broad range of apple juice concentrations. The tAb used in the ELISA test, shown in Table 1, agrees with that used in the PEG–AuNP-based method. For 59° Brix apple juice, ELISA test results showed negative results irrespective of the presence of *Z. rouxii* B-WHX-54. The reason may be that *Z.*

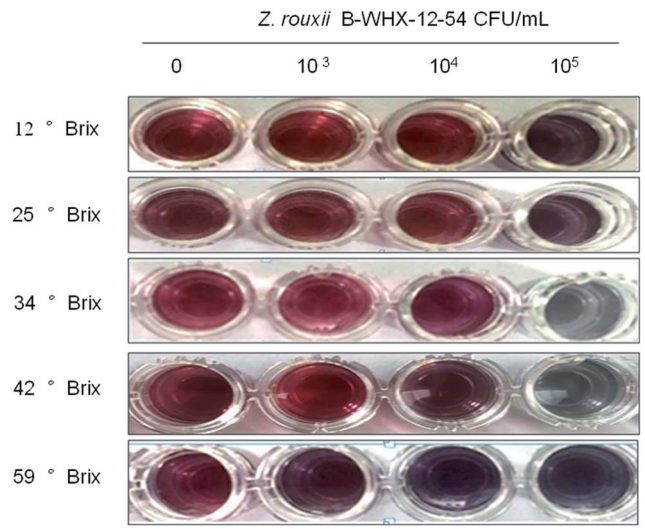

Fig. 7 The naked eye observations of wash-free immunoassay (tAb–PEG–AuNPs) for *Z. rouxii* at different concentrations of apple juice.

Table 1 Samples measured by conventional indirect ELISA using tAb

	Z. rouxii B-WHX-54			
ELISA	0	10^3	10^4	10^5
12° Brix	−(0.1)[a]	−(0.10)	−(0.11)	−(0.20)
25° Brix	−(0.21)	−(0.21)	−(0.24)	−(0.24)
34° Brix	−(0.218)	−(0.244)	−(0.24)	+(0.34)[b]
42° Brix	−(0.22)	−(0.23)	−(0.24)	+(0.36)
59° Brix	−(0.19)	−(0.22)	−(0.21)	−(0.22)

[a] Negative. [b] Positive.

Table 2 Comparison between our method and conventional ELISA method

Category	Wash-free immunoassay	Conventional ELISA
Time of fabrication	Preparation of PEG linker: 2–3 days. Preparation of Ab–PEG–AuNPs: less than 1 day	Preparation of blocking buffer, washing buffer, incubation buffer, tetramethylbenzidine (TMB) reagents and termination solution: about 1 day
Time of analysis	About 30 min	About 6 h
Amount of reactive	3 μL	100 μL
Main advantages	Rapid simple	Quantitative widely applied
Analytical characteristics	Rapid no skills required readable by naked eye	Readout *via* spectrophotometer

rouxii will float on the surface of 59° Brix apple juice because of the high viscosity of concentrated juice. Therefore, *Z. rouxii* B-WHX-54 cannot attach to the bottom of 96-well polystyrene microplates (Fig. S4†), exhibiting negative results. However, tAb–PEG–AuNPs will inevitably cross-react when the molecular concentration is sufficiently large or the viscosity affects the Au growth in the analysis system, so that the wash-free immunoassay shows a positive result regardless of the presence of targets. Unambiguously, tAb–PEG–AuNPs might hold promising advantages for the determination of *Z. rouxii* in apple juice (Fig. S4†). In addition, the detailed comparison of the AuNP-based method and ELISA method shown in Table 2 help developers make proper choices.

Based on these results, we indicate that antibodies are the key factor in the wash-free immunoassay when this method is applied for the detection of other food spoilage microbes. Compared with other methods for detecting spoilage microbes, ELISA[6] demanded tedious wash steps, E-nose[13] and RT-PCR[30] required high personal skills, and the plating[31] method was time consuming; conversely, the established method in our study was simple, sensitive and fast. Thus, it has great potential for detecting other food spoilage microorganisms.

Conclusion

The wash-free immunoassay strategy based on AuNP-growth can be applied in rapid detection of *Z. rouxii* in apple juice. The polyclonal antibodies were assembled on AuNPs to recognize the cell surface antigens of *Z. rouxii*. Upon addition of Au growth solutions, the inter-particle spacing of Ab–PEG–AuNP on the cell surface of *Z. rouxii* was reduced depending on the Au growth, leading to an optical transition. Therefore, the color change of the analysis system was observed by simply mixing real samples and Ab–PEG–AuNP solutions, followed by addition of Au growth solutions. This method does not need tedious wash steps, the involvement of any enzyme and the separation of targets. The concept used in this study can be expanded to food spoilage microbe detection and only requires to change the Ab in the Ab–PEG–AuNP probe.

Acknowledgements

This study was financially supported by the Shaanxi Special Project of China (2016KTCQ03-12), the National Natural Science Foundation of China (31371814, 31671866), and the Scientific and Technology Cooperation Project in Hongkong, Macao and Taiwan of China (2015DFT30130).

References

1 B. K. Kumar, P. Raghunath, D. Devegowda, V. K. Deekshit, M. N. Venugopal, I. Karunasagar and I. Karunasagar, *Int. J. Food Microbiol.*, 2011, **145**, 244–249.
2 C. Pastells, G. Acosta, N. Pascual, F. Albericio, M. Royo and M. P. Marco, *Anal. Chim. Acta*, 2015, **889**, 203–211.
3 Z. Wang, R. Cai, Y. Yuan, C. Niu, Z. Hu and T. Yue, *Int. J. Food Microbiol.*, 2014, **175**, 30–35.
4 W. Xu, J. Wang and Q. Li, *FEMS Yeast Res.*, 2014, **14**, 1273–1285.
5 J. Li, K. Xia and C. Yu, *Food Control*, 2013, **30**, 251–254.
6 J. Li, R. Huang, K. Xia and L. Liu, *Food Control*, 2014, **40**, 172–176.
7 H. Song, H. Xue and Y. Han, *Food Control*, 2011, **22**, 883–887.
8 H. Liu, P. Rong, H. Jia, J. Yang, B. Dong, Q. Dong, C. Yang, P. Hu, W. Wang and H. Liu, *Theranostics*, 2016, **6**, 54–64.
9 X. M. Nie, R. Huang, C. X. Dong, L. J. Tang, R. Gui and J. H. Jiang, *Biosens. Bioelectron.*, 2014, **58**, 314–319.
10 X. Bai, C. Shao, X. Han, Y. Li, Y. Guan and Z. Deng, *Biosens. Bioelectron.*, 2010, **25**, 1984–1988.
11 J.-S. Lee, P. A. Ulmann, M. S. Han and C. A. Mirkin, *Nano Lett.*, 2008, **8**, 529–533.
12 J. Liu and Y. Lu, *J. Am. Chem. Soc.*, 2003, **125**, 6642–6643.
13 H. Wang, Z. Hu, F. Long, C. Guo, Y. Yuan and T. Yue, *Int. J. Food Microbiol.*, 2016, **217**, 68–78.
14 T. C. Dakal, L. Solieri and P. Giudici, *Int. J. Food Microbiol.*, 2014, **185**, 140–157.
15 J. Watanabe, K. Uehara and Y. Mogi, *Genetics*, 2013, **195**, 393–405.
16 H. Wang, Z. Hu, F. Long, C. Niu, Y. Yuan and T. Yue, *J. Food Sci.*, 2015, **80**, M1850–M1860.
17 H. Guo, C. Niu, B. Liu, J. Wei, H. Wang, Y. Yuan and T. Yue, *Int. J. Food Microbiol.*, 2016, **233**, 44–51.
18 Z. Wang, T. Yue, Y. Yuan, R. Cai, C. Guo, X. Wang and C. Niu, *J. Food Sci.*, 2012, **77**, M643–M649.
19 J. Cui, K. Zhang, Q. Huang, Y. Yu and X. Peng, *Anal. Chim. Acta*, 2011, **688**, 84–89.
20 M. Casanova, M. L. Gil, L. Cardeñoso, J. P. Martinez and R. Sentandreu, *Infect. Immun.*, 1989, **57**, 262–271.
21 J. Turkevich, P. C. Stevenson and J. Hillier, *Discuss. Faraday Soc.*, 1951, **11**, 55–75.

22 Z. Wang, T. Yue, Y. Yuan, R. Cai, C. Guo, X. Wang and C. Niu, *J. Food Sci.*, 2012, **77**(11), M643–M649.
23 A. Beaussart, D. Alsteens, S. El-Kirat-Chatel, P. N. Lipke, S. Kucharíková, P. Van Dijck and Y. F. Dufrêne, *ACS Nano*, 2012, **6**(12), 10950–10964.
24 W. Eck, G. Craig, A. Sigdel, G. Ritter, L. J. Old, L. Tang, M. F. Brennan, P. J. Allen and M. D. Mason, *ACS Nano*, 2008, **2**, 2263–2272.
25 J.-Y. Byun, Y.-B. Shin, D.-M. Kim and M.-G. Kim, *Analyst*, 2013, **138**, 1538–1543.
26 H. Hoffmann, S. Baldofski, K. Hoffmann, S. Flemig, C. P. Silva, V. I. Esteves, F. Emmerling, U. Panne and R. J. Schneider, *Talanta*, 2016, **158**, 198–207.
27 Z. Wang, R. C. Beier, Y. Sheng, S. Zhang, W. Jiang, Z. Wang, J. Wang and J. Shen, *Anal. Bioanal. Chem.*, 2013, **405**, 4027–4037.
28 Y.-Y. Hsieh, P.-H. Hung and J.-Y. Leu, *Molecular Cell*, 2013, **50**, 82–92.
29 H. J. Kim, H. R. Lee, C. S. Kim, Y. S. Jin and J. H. Seo, *Enzyme Microb. Technol.*, 2013, **53**, 174–180.
30 H. Rawsthorne and T. G. Phister, *Int. J. Food Microbiol.*, 2006, **112**, 1–7.
31 H. Wang, Z. Hu, F. Long, C. Guo, Y. Yuan and T. Yue, *J. Food Prot.*, 2015, **78**, 2052–2063.